PAN
ARCHIVES OF ACOUSTICS
Vol. **45**, No. 1, pp. 85–92 (2020)
DOI: 10.24425/aoa.2020.132484



## Research Paper

# Analysis of the Room Acoustic with Impedance Boundary Conditions in the Full Range of Acoustic Frequencies

Edyta PRĘDKA*, Adam BRAŃSKI

*Department of Complex Systems*
*Faculty of Electrical and Computer Engineering Technical University of Rzeszow*
al. Powstańców Warszawy 12, 35-959 Rzeszow, Poland
*Corresponding Author e-mail: edytap@prz.rzeszow.pl

(*received April 16, 2019; accepted December 10, 2019*)

An efficiency of the nonsingular meshless method (MLM) was analyzed in an acoustic indoor problem. The solution was assumed in the form of the series of radial bases functions (RBFs). Three representative kinds of RBF were chosen: the Hardy's multiquadratic, inverse multiquadratic, Duchon's functions. The room acoustic field with uniform, impedance walls was considered. To achieve the goal, relationships among physical parameters of the problem and parameters of the approximate solution were first found. Physical parameters constitute the sound absorption coefficient of the boundary and the frequency of acoustic vibrations. In turn, parameters of the solution are the kind of RBFs, the number of elements in the series of the solution and the number and distribution of influence points. Next, it was shown that the approximate acoustic field can be calculated using MLM with a priori error assumed. All approximate results, averaged over representative rectangular section of the room, were calculated and then compared to the corresponding accurate results. This way, it was proved that the MLM, based on RBFs, is efficient method in description of acoustic boundary problems with impedance boundary conditions and in all acoustic frequencies.

**Keywords:** architectural acoustic; meshless method; radial bases functions; impedance boundary condition.

## 1. Introduction

One of the main aim of the room acoustics is the description of the acoustic field. The room acoustics is determined by its geometry and sound absorption of walls (Kuttruff, 2000; Pilch, Kamisiński, 2011; Rubacha *et al.*, 2012; Kamisiński, 2012; Kamisiński *et al.*, 2016). Depending on the acoustic frequency, there are three groups of methods describing the room acoustics, i.e.: wave-based methods (WBM) (Meissner, 2009; 2016b; Kamisiński *et al.*, 2016; Siltanen *et al.*, 2010), image source methods (ISM) (Suh, Nelson, 1999; Aretz *et al.*, 2014; Boucher *et al.*, 2016) and acoustics energy methods (AEM) (Meissner, 2013). In general, WBM is used for low frequencies, ISM for the early part of the room response for middle and high frequencies and AEM for the rest of the response for middle and high frequencies. Each method has advantages and disadvantages; some of them are enumerated in (Brański, Prędka, 2018). These different groups of methods have some links among them (Rindel, 2010) and in some frequency ranges they can be applied interchangeably.

As can be seen, there is not one method which may be applied in full range of acoustic frequencies. Although this gap is partially filled by hybrid methods, but it is not convenient from a numerical point of view. So, it is necessary to search of the general method that would be effective for all acoustic frequencies. This problem is partially solved by this paper.

Such a method ought to be searched among WBM; other two methods, i.e. ISM and AEM, are not suitable for describing the field in full acoustic frequencies, (Brański, Prędka, 2018) and references cited therein. The finite element method (FEM) (Fish, Belytschko, 2007; Dobrucki *et al.*, 2010; Shojaei *et al.*, 2019), the boundary element method (BEM) (Sladek *et al.,* 2000; Brański *et al.*, 2012; Borkowski, 2015; Brański, Borkowska, 2015a; 2015b) and MLM are of great importance among

WBM. But the number, distribution and construction of elements both in FEM and BEM is a difficult problem.

To avoid this problem, researchers are currently focusing on MLM (Atluri, 2004; Antunesp, Valtchen, 2010; Chen *et al.*, 2013; Fu *et al.*, 2014; Majkut, Olszewski, 2014; Shojaei, 2016; Bajko *et al.*, 2017; Brański, Prędka, 2018). The MLM bases on the solution of the boundary problem in the form of series, in which bases are RBFs and unknown coefficients, which are interpreted as intensities of influence points. In classical formulation of the problem, unknown coefficients are obtained by collocation method. Although the number and distribution of both influence points and collocation ones play significant role this problem is not considered in the paper and it remains an open issues (Shojaei *et al.*, 2019).

The purpose of this study is to apply MLM and analyze its effectiveness to solve the internal acoustic problem with impedance boundary conditions imposed on walls (Brański *et al.*, 2017) and in full range of acoustic frequencies. For this purpose, three types of RBFS are tested: Hardy multi-square (Prędka, 2016; Brański, Prędka, 2018), inverse multiquadratic (Brański, Prędka, 2017), Duchon's (Duchon, 1976).

The first two RBFs depend on the shape parameter. So, in this paper the value of the shape parameter is analyzed as a function of frequency, sound absorption coefficient and number of influence points, especially an influence of frequency on the shape parameter is analyzed. For all RBFs, an influence of frequency on the number of series elements is analyzed too. In this way, all parameters of the solution are determined in the function of physical parameters. It should be highlighted, that all calculations are performed on an assumption that the error between an average exact acoustic field and an average approximate acoustic field in the domain is less than 5%. Finally, by selecting some physical parameters of the boundary problem, distributions of approximate and accurate acoustic fields are compared (Brański *et al.*, 2017).

This way it is proved that MLM can be a powerful tool for analyzing of the room acoustic with impedance boundary conditions and it is useful in the full range of acoustic frequencies.

## 2. Exact theory of the boundary acoustic problem

Details of this theory were presented in (Brański, Prędka, 2018). Here, only necessary equations, figures and symbols are quoted in order to the article should be a separate whole and the reader could understand its content.

The problem is considered in the domain $\Omega$ with the boundary $\Gamma$ and the mathematical model is described by the wave equation and acoustic boundary conditions. In steady state the problem is described by the Helmholtz differential equation and acoustic boundary conditions. The Helmholtz equation is,

$$\mathsf{L}u(\mathbf{x}) = \Delta u(\mathbf{x}) + k_f^2 u(\mathbf{x}) = f(\mathbf{x}), \qquad \mathbf{x} = \mathbf{x}' \in \Omega, \quad (1)$$

where $u(\mathbf{x})$ is the acoustic potential, $k_f$ – the wave number, $k_f = \omega_f/c$, $\omega_f = 2\pi f$ – the angular exciting frequency $f$, $f(\mathbf{x})$ – the given function; it represents an acoustic source and in 2D it is given by $f(\mathbf{x}) = A H_0^{(2)}(k_f r)$, i.e., the 0-order, Hankel function of the second kind (Mclachlan, 1964), $A$ is an intensity of the source.

The acoustic pressure described with the acoustic potential $u(\mathbf{x})$ takes the form

$$p(\mathbf{x}) = i\rho\omega u(\mathbf{x}), \quad (2)$$

where $\rho$ is the air density, $i = \sqrt{-1}$.

Regarding acoustic boundary conditions, for practical case, the floor is described through the Neumann boundary condition ($\mathbf{N}$), but walls and ceiling are modeled through impedance Robin boundary conditions ($\mathbf{R}$), $\Gamma = \mathbf{N} \cup \mathbf{R}$; the cross section of this problem is depicted in Fig. 1, so one has,

$$D_n u(\mathbf{x}) = 0, \qquad \mathbf{x} \in \mathbf{N}, \quad (3)$$

$$D_n u(\mathbf{x}) + z_0 u(\mathbf{x}) = 0, \qquad \mathbf{x} \in \mathbf{R}, \quad (4)$$

where $z_0(\mathbf{x}) = (\omega\rho)/z(\mathbf{x})$.

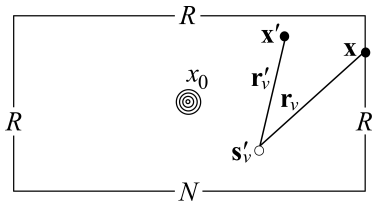


Fig. 1. Cross section of the acoustic problem.

The $z(\mathbf{x})$ is the acoustic impedance and in fact, it is the impedance of any material and it is expressed via the absorption coefficient $\alpha(\mathbf{x})$ (Meissner, 2016a; Piechowicz, Czajka, 2012). Both $\alpha(\mathbf{x})$ and $z(\mathbf{x})$ are connected to each other by the formula (Kuttruff, 2000),

$$z(\mathbf{x}) = \rho c \frac{1 + (1 - \alpha(\mathbf{x}))^{1/2}}{1 - (1 - \alpha(\mathbf{x}))^{1/2}}. \quad (5)$$

## 3. Discrete theory of the boundary acoustic problem

The discretization is done by domain-boundary MLM. The approximate solution of the problem is assumed as the series,

$$\widetilde{u}(\mathbf{x}') = \sum_{\nu} a_\nu, \mathsf{R}(r'_\nu), \qquad r'_\nu = |\mathbf{s}_\nu - \mathbf{x}'|, \quad (6)$$

where $a_\nu$ are certain coefficients and remain to be calculated, $\mathsf{R}(r_\nu)$ – radial bases functions (RBFS), $\mathbf{s}_\nu \in \overline{\Omega} = \Omega \cup \Gamma$, $\mathbf{x}' \in \Omega$, Fig. 1.

The main advantages and drawbacks of RBFs were enumerated in (Brański, Prędka, 2018). In the paper, three kinds of RBFS are considered (Figs 2–4):

- Hardy's multiquadratic (Hardy, 1971; Prędka, 2016; Brańki, Prędka, 2018), Fig. 2,

$$\mathsf{R}(r) = (-1)^{\lceil\beta\rceil}(C^2+r^2)^\beta, \quad C>0, \quad \beta>0, \quad \beta \notin N, \tag{7}$$

  where $\lceil\beta\rceil$ means the smallest integer larger than $\beta$.
- Inverse multiquadratic (Brański, Prędka, 2017), Fig. 3,

$$\mathsf{R}(r) = (C^2+r^2)^{-\beta}, \quad C>0, \quad \beta>0. \tag{8}$$

- Duchon's (Duchon, 1976; Cheng, 2000), Fig. 4,

$$\mathsf{R}(r) = (-1)^{\beta+1} r^{2\beta} \log r, \quad \beta \in N. \tag{9}$$

  For $\beta = 1$ in 2D space these functions are called thin plate splines (Cheng, 2000).

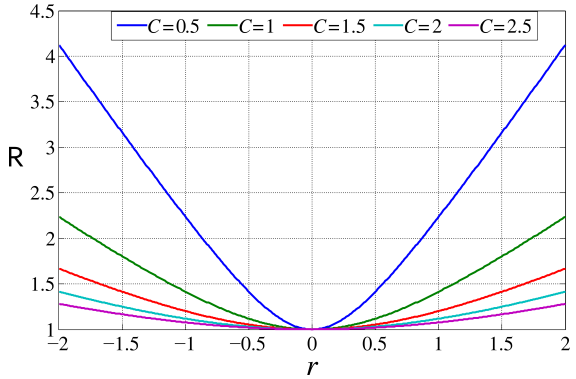


Fig. 2. Hardy's multiquadratic RBF for different values of the shape parameter $C$.

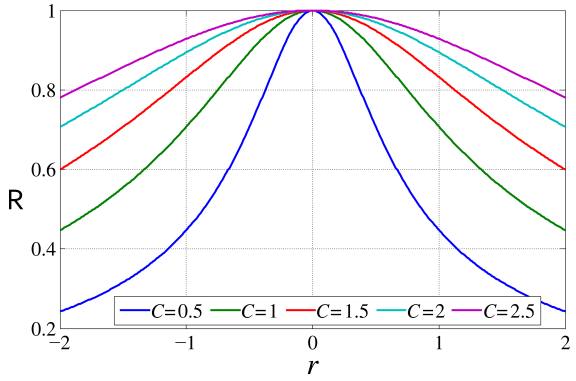


Fig. 3. Inverse multiquadratic RBF for different values of the shape parameter $C$.

As can be seen from Figs 2–4, different shapes of $\mathsf{R}(r)$ are chosen. Furthermore, to make useful the first two $\mathsf{R}(r)$, the shape coefficient $C$ must be determined.

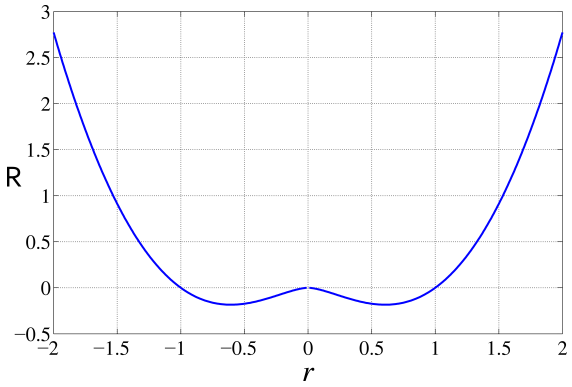


Fig. 4. Duchon's RBF, $\beta = 1$.

To calculate $a_\nu$ in Eq. (6), the solution $\widetilde{u}(\mathbf{x}')$ substitutes to equations describing the problem Eqs (1), (3), and (4). Hence, instead of Eq. (1) is

$$\sum_\nu a_\nu \left(D_x^2\mathsf{R}(r'_{\nu\mu}) + D_y^2\mathsf{R}(r'_{\nu\mu}) + k^2\mathsf{R}(r'_{\nu\mu})\right) = f(\mathbf{x}'_\mu). \tag{10}$$

Derivatives $D_x^2(\cdot)$ and need explanation; since $r'_{\nu\mu} = |\mathbf{s}_\nu - \mathbf{x}'_\mu|$, then in $D_x^2(\cdot)$, the derivative with respect to $x$ should be understand as derivative with respect to $x'_\mu$ and so on. The intensity $A$ is chosen, so that $L_m$ takes the same value for different values of the absorption coefficient $\alpha$ and frequency $f$.

The Neumann, Eq. (3), and the Robin, Eq. (4), boundary conditions are given respectively by

$$\sum_\nu a_\nu D_{\mathbf{n}}\mathsf{R}(r_{\nu\mu}) = 0, \quad \mathbf{x}_\mu \in \mathbf{N}, \tag{11}$$

$$\sum_\nu a_\nu \left(D_{\mathbf{n}}\mathsf{R}(r_{\nu\mu}) + z_0(\mathbf{x}_\mu)\mathsf{R}(r_{\nu\mu})\right) = 0, \quad \mathbf{x}_\mu \in \mathbf{R}. \tag{12}$$

In Eqs (11) and (12), the versor $\mathbf{n}$ is defined at $x_\mu$, it is perpendicular to the boundary $\Gamma$ and is directed outside the domain $\Omega$, for example, if $\mathbf{x}_\mu \in \mathbf{N}$, $D_{\mathbf{n}}(\cdot) = -D_y(\cdot)$ and so on.

## 4. Relationships among physical parameters and parameters of the approximate solution

First, the acoustic pressure is calculated via Eq. (2) and next, the value of the sound pressure level at point $\mathbf{x} = \mathbf{x}' \in \Omega$ is calculated by

$$L(\mathbf{x}) = 10\log\left(\frac{p(\mathbf{x})}{p_0}\right)^2, \tag{13}$$

where $p_0 = 2\cdot 10^{-5}$ Pa.

To notice quantitative change of $L(\mathbf{x})$ in the domain $\Omega$, the mean value ought to be calculated based on the equation,

$$p_m = \frac{1}{n_i}\sum_i p(\mathbf{x}_i), \qquad L_m = 10\log\left(\frac{p_m}{p_0}\right)^2, \tag{14}$$

where $i = 1, 2, ..., n_i$ is the number of calculated points $\mathbf{x}_i = \mathbf{x}'_i \in \Omega$.

Hereunder all calculations are made on the basis of the formula

$$\varepsilon = \left| \frac{(L_m - \widetilde{L}_m)}{L_m} \right| \cdot 100\%, \tag{15}$$

where $\widetilde{L}_m$ is an approximate solution, $L_m$ – the exact one (Brańśki *et al.*, 2017).

The intensity of the source $A$ is chosen, so that $L_m$ takes the same value for different values of the absorption coefficient $\alpha$ and the frequency $f$.

Following global values and symbols are assumed: $\rho = 1.205\ \mathrm{kg/m^3}$, $c = 344\ \mathrm{m/s}$, $\{a_x, b_x\} = \{0, 5\}$ m, $\{a_y, b_y\} = \{0, 2.5\}$ m. The source is placed at the point $\mathbf{x}_0 = \{x_0, y_0\} = \{2.5, 1.25\}$ m. Furthermore, based on Eqs (3) and (4), the acoustic values $z_0(a_x) \equiv z_0(b_x) \equiv z_0(b_y) = Z$ and $z_0(a_y) = 0$ are imposed on the boundaries. Influence points are marked by "○" and collocation points are marked by "•". Both kinds of points cover each other; the rest of symbols are depicted in Fig. 5.

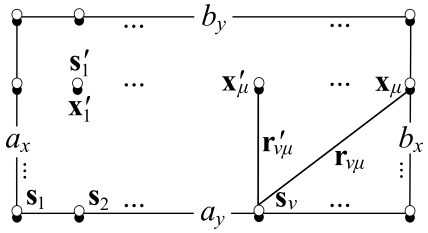


Fig. 5. Distribution of all points in the $\overline{\Omega}$.

Below, details of numerical calculations are presented for discrete values of the full scope of the absorption coefficient, i.e. $\{\alpha\} = \{0.1, \text{step}\,0.1, 0.9\}$ and full range of the acoustic frequency, represented by octave frequencies, namely $\{f\} = \{125, 250, 500, 1000\ 2000, 4000, 8000, 16000\}$ Hz.

To attain the aim of the paper, three kinds of calculations are carried out.

1) First, the relationship between the parameter $C$ and the absorption coefficient $\alpha$ is found for different values of frequency $f$ and different number of elements $n$ of the series; results are shown below:

   - Hardy's multiquadratic RBF (Fig. 6),
   - inverse multiquadratic RBF (Fig. 7).

   From analysis of Figs 6 and 7 follows that the parameter $C$ does not depend on the coefficient $\alpha$. But it strongly depends on frequency $f$; it is analyzed in the next step.

2) An influence of frequency $f$ on the shape parameter $C$ is analyzed:

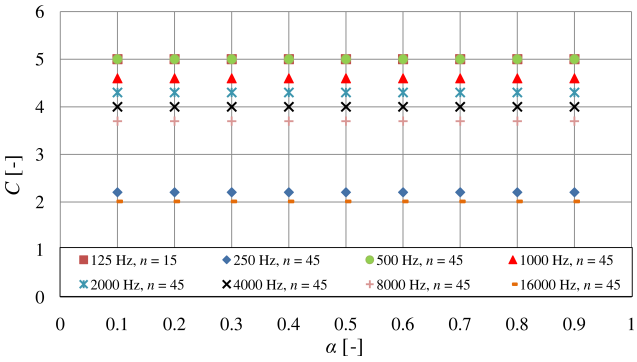


Fig. 6. Shape parameter $C$ as the function of the absorption coefficient $\alpha$ for Hardy's multiquadratic RBF.

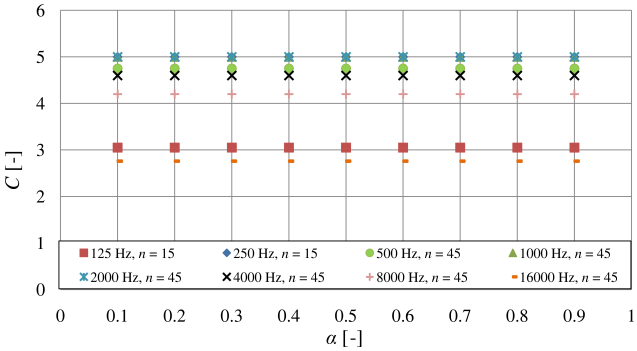


Fig. 7. Shape parameter $C$ as the function of the absorption coefficient $\alpha$ for inverse multiquadratic RBF.

   - Hardy's multiquadratic RBF; points marked as "○" are the arithmetic average calculated for $C$ corresponding to different values of the number of influence points$n$; the red curve is the approximation of the mean values by the function: $C = a_1 + a_2/f$ where $a_1 = 1.9753$, $a_2 = 388.0844$. Results are given belowm
   - inverse multiquadratic RBF – quite similar as in the previous case, mean values of the parameter $C$is approximated by the function: $C = a_1 + a_2/f$ where $a_1 = 1.5019$ and $a_2 = 465.4814$; see results below.

   Figures 8 and 9 show possibility of reading the value of the shape parameter $C$ for given frequency $f$. However, this approximation does not take into account an influence of frequency $f$ on the number of elements of the series $n$. This problem is investigated in the next point.

3) An influence of frequency $f$ on the number of elements of the series $n$ is analyzed for all three RBFs; results are shown below:

   - Hardy's multiquadratic RBF (Fig. 10),
   - inverse multiquadratic RBF (Fig. 11),
   - Duchon's RBF (Fig. 12).

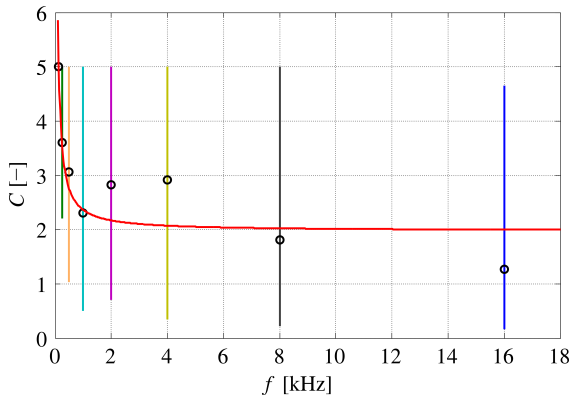


Fig. 8. Shape parameter $C$ as the function of frequency $f$ for Hardy's multiquadratic RBF.

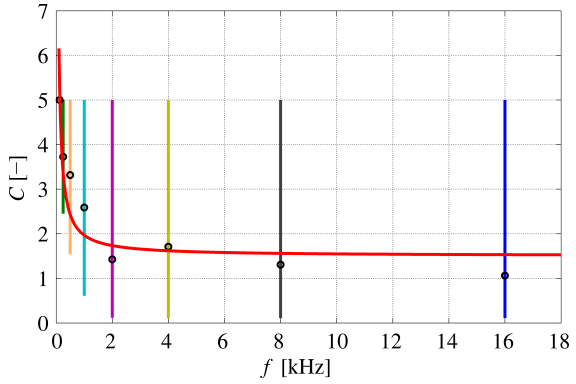


Fig. 9. Shape parameter $C$ as the function of frequency $f$ for inverse multiquadratic RBF.

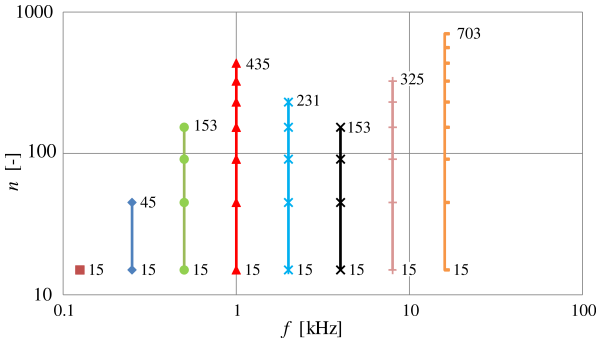


Fig. 10. Number of elements $n$ as the function of frequency $f$ for Hardy's multiquadratic RBF.

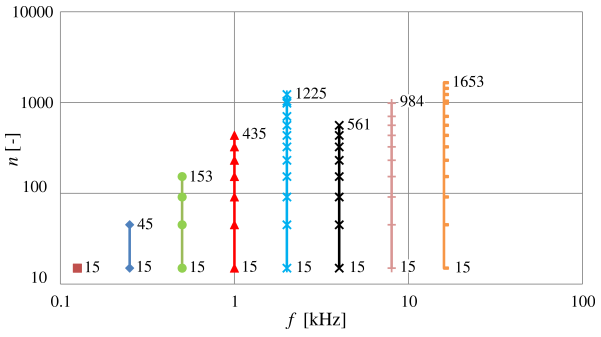


Fig. 11. Number of elements $n$ as the function of frequency $f$ for inverse multiquadratic RBF.

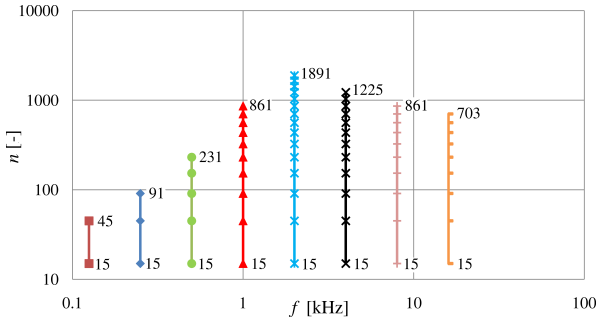


Fig. 12. Number of elements $n$ as the function of frequency $f$ for Duchon's RBF.

Analyzing Figs 10–12, it can be seen that for all tested RBFs and for $n$ = 15, results are achieved with the assumed accuracy $\varepsilon \leq 5\%$. However, the different number of points $n$ is also possible. But then, in the case of parameterized RBFS, change of the parameter $C$ should be included; this problem will be solved in the separate article.

Below, to confirm previous research results, some numerical examples are joined.

## 5. Numerical calculations, results, conclusions

Numerical calculations concern the distribution of the acoustical field, in $L(\mathbf{x})$ [dB], Eq. (13), in the cross section of the domain, Fig. 5. Results presented below are only for extreme values of physical parameters, i.e. 250 Hz, $\alpha$ = 0.1 and 2000 Hz, $\alpha$ = 0.9. Exact results are depicted on the left side, but approximation ones (RBFS solutions), are on the right side. Results are presented only for Duchon's RBF. This is because, in the case of other two RBFS functions similar results are obtained.

As can be seen from Figs 13 and 14, for low frequencies and low absorption coefficients, approximated MLM solution provides only the same average $L_m$ in the cross section domain. However, for higher frequencies and higher absorption coefficients, in addition to the previous conclusion, shapes of acoustic fields are similar.

## 6. Conclusions

The paper proposes MLM, based on three representative RBFs, to the solution of the acoustic boundary problem with uniform impedance boundary conditions imposed on walls. First, for Hardy's multiquadratic RBF and inverse multiquadratic RBF, the relationship between the shape parameter $C$ and the absorption coefficient $\alpha$ is found for different values of frequency $f$ and the different number of elements $n$ in the series. It has been demonstrate, that coefficient $C$ does not depend on the absorption coefficient $\alpha$, but it strongly depends on the frequency $f$.

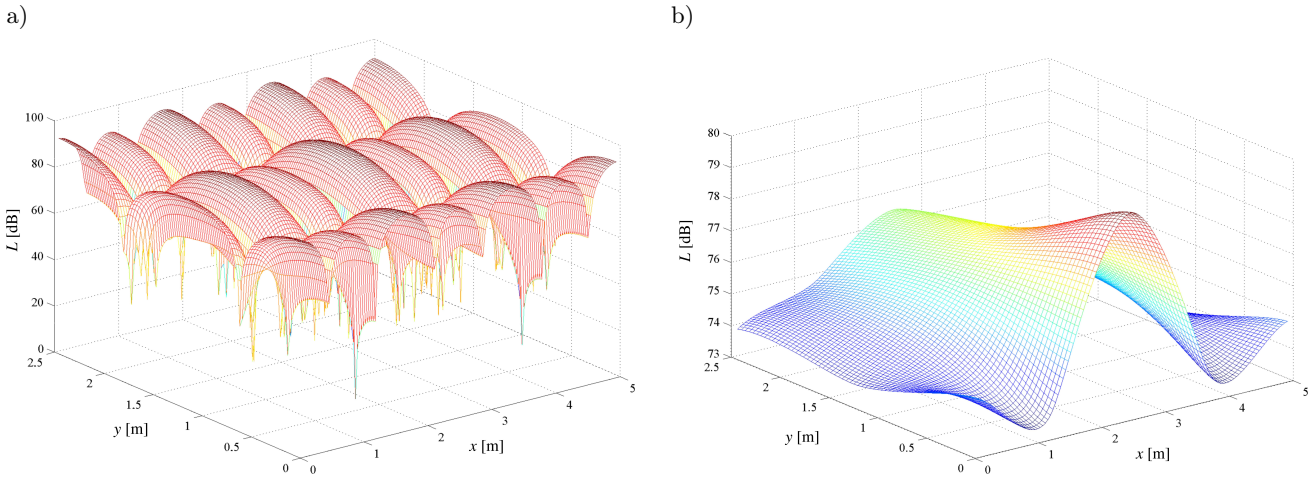


Fig. 13. Distribution of the acoustical field for 250 Hz, $\alpha = 0.1$ (LHS – exact, RHS – approximated): a) $L_m = 75.00$ dB, b) $L_m = 75.61$ dB.

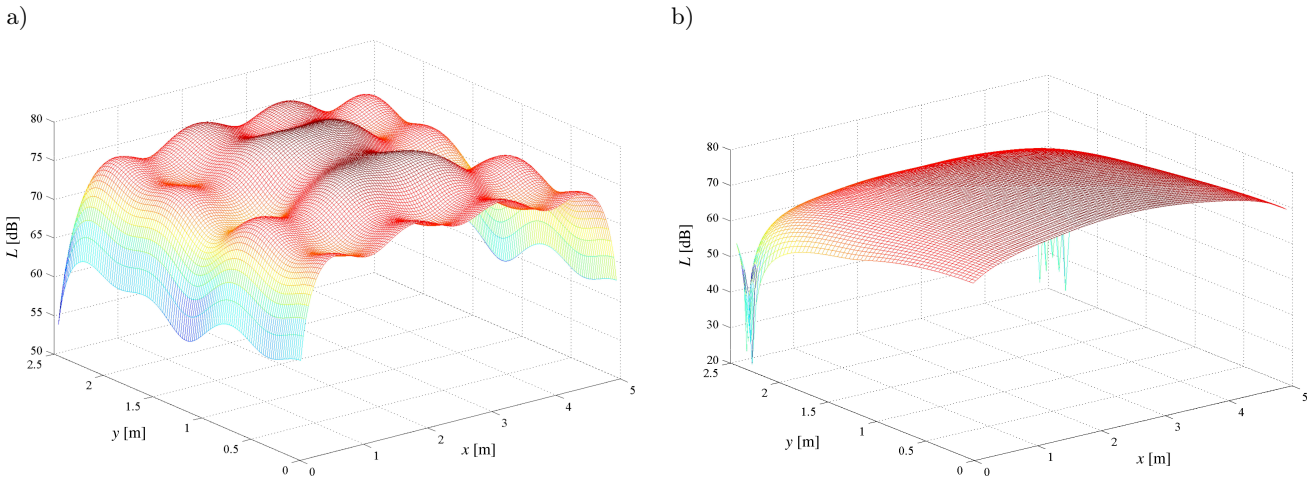


Fig. 14. Distribution of the acoustical field for 2000 Hz, $\alpha = 0.9$ (LHS – exact, RHS – approximated): a) $L_m = 74.77$ dB, b) $L_m = 73.22$ dB.

So, an influence of frequency $f$ on the shape parameter $C$ is analyzed. It has been proved, that this influence is hyperbolic, but different for Hardy's multiquadratic RBF and inverse multiquadratic RBF. In this calculation, the course of the hyperbolic curve does not take into account the influence of frequency $f$ on the number of elements $n$ in the series.

Then, this problem is analyzed for all three RBFs. It has been proved that, for all tested RBFs, even 15 elements of the series ensure results with assumed accuracy $\varepsilon \leq 5\%$.

To verify an efficiency of MLM, the acoustic field in the cross section of the domain has been also calculated. It has been noted, that for all acoustic frequencies and all absorption coefficients, MLM ensures the correct average value of the acoustic field; this conclusion ought to be very useful in the architectural acoustic. Furthermore, for higher frequencies and higher absorption coefficients, MLM properly also describes the distribution of the acoustic field in the domain.

In the future, based on average value of the acoustic field in the domain and minimizing accuracy $\varepsilon$, an efficiency of MLM will be further analyzed especially at low frequencies and low absorption coefficients. Particular attention will also be paid to the distribution of the acoustic field in the domain.

## References

1. Antunesp R.S., Valtchev S.S. (2010), A meshfree numerical method for acoustic wave propagation problems in planar domains with corners and cracks, *Journal of Computational and Applied Mathematics*, **234**(9): 2646–266, doi: 10.1016/j.cam.2010.01.031

2. Aretz M., Dietrich P., Vorländer M. (2014), Application of the mirror source method for low frequency sound prediction in rectangular rooms, *Acta Acustica united with Acustica*, **100**(2): 306–319, doi: 10.3813/AAA.918710

3. Atluri S.N. (2004), *The meshless method (MLPG) for domain & BIE discretization*, Tech Science Press, Forsyth, GA, USA.
4. Bajko J., Niedoba P., Cermak L., Cham J.I. (2017), *Simulation of the acoustic wave propagation using a meshless method*, EPJ Web of Conferences 143, 02003, EFM 2016, doi: 10.1051/epjconf/201714302003.
5. Borkowski M. (2015), 2D capacitance extraction with direct boundary methods, *Engineering Analysis with Boundary Elements*, **58**: 195–201, doi: 10.1016/j.enganabound.2015.04.017.
6. Boucher M., Pluymers B., Desmet W. (2016), Interference effects in phased beam tracing using exact half-space solutions, The Journal of the Acoustical Society of America, **140**(6): 4204–4212, doi: 10.1121/1.4971283
7. Brański A., Borkowska D. (2015a), Effectiveness of nonsingular solution of the boundary problems based on Trefftz methods, Engineering Analysis with Boundary Elements, **59**: 97–104, doi: 10.1016/j.enganabound.2015.04.016.
8. Brański A., Borkowska D. (2015b), Galerkin versions of nonsingular Trefftz methods derived from variational formulations for 2D Laplace problem, *Acta Physica Polonica A*, **128**(1A): A50–A55, doi: 10.12693/APhysPolA.128.A-50.
9. Brański A., Borkowski M., Borkowska D. (2012), A comparison of boundary methods based on inverse variational formulation, *Engineering Analysis with Boundary Elements*, **36**(4): 505–510, doi: 10.1016/j.enganabound.2011.11.004.
10. Brański A., Kocan-Krawczyk A., Prędka E. (2017), An influence of the wall acoustic impedance on the room acoustics. The exact solution, *Archives of Acoustics*, **42**(4): 677–687, doi: 10.1515/aoa-2017-0070.
11. Brański A., Prędka E. (2017), Effectiveness of the inverse multi-quadratic RBF in acoustic indoor problem, *Open Seminar on Acoustics*, Gliwice, 55–58.
12. Brański A., Prędka E. (2018), Nonsingular meshless method in an acoustic indoor problem, *Archives of Acoustics*, **43**(1): 75–82, doi: 10.24425/118082.
13. Chen W., Fu Z., Zhang C.Z. (2013), *Recent advances on radial function collocation methods*, Springer, Berlin.
14. Cheng A.H.-D. (2000), Particular solutions of Laplacian, Helmholtz-type, and polyharmonic operators involving higher order radial basis functions, *Engineering Analysis with Boundary Elements*, **24**(7–8): 531–538, doi: 10.1016/S0955-7997(00)00033-3.
15. Dobrucki A., Żółtogórski B., Pruchnicki P., Bolejko R. (2010), Sound-absorbing and insulating enclosures for ultrasonic range, *Archives of Acoustics*, **35**(2): 157–164.
16. Duchon J. (1976), *Splines minimizing rotation invariant semi-norms in Sobolev spaces, Lecture notes in mathematics*, Vol. 571, pp. 85–110, Springer, New York.
17. Fish J., Belytschko T. (2007), *A first course in finite element elements*, John Wiley & Sons.
18. Fu Z.-J., Chen W., Chen J.-T., Qu W.-Z. (2014), Singular boundary method: three regularization approaches and exterior wave applications, *CMES: Computer Modeling in Engineering & Sciences*, **99**(5): 417–443, doi: 10.3970/cmes.2014.099.417.
19. Hardy R.L. (1971), Multiquadric equations of topography and other irregular surfaces, *Journal of Geophysical Research*, **76**(8): 1905–1915, doi: 10.1029/JB076i008p01905.
20. Kamisiński T. (2012), Correction of acoustics in historic opera theatres with the use of Schroeder diffuser, *Archives of Acoustics*, **37**(3): 349–354.
21. Kamisiński T., Kulowski A., Kinasz R. (2016), Can historic interiors with large cubature be turned acoustically correct?, *Archives of Acoustics*, **41**(1): 3–14, doi: 10.1515/aoa-2016-0001.
22. Kuttruff H. (2000), *Fundamentals of physical acoustics. Room acoustic*, Wiley–Interscience, New York.
23. Majkut L., Olszewski R. (2014), Acoustic eigenanalysis with radial basis functions, *Acta Physica Polonica A*, **125**(4A): 77–82, doi: 10.12693/APhysPolA.125.A-7.
24. Meissner M. (2009), Computer modelling of coupled spaces: variations of eigenmodes frequency due to a change in coupling area, *Archives of Acoustics*, **34**(2): 157–168.
25. Meissner M. (2013), Evaluation of decay times from noisy room responses with puretone excitation, *Archives of Acoustics*, **38**(1): 47–54.
26. Meissner M. (2016a), Improving acoustics of hard-walled rectangular room by ceiling treatment with absorbing material, *Progress of Acoustics*, Polish Acoustical Society, Warsaw Division, Warszawa–Białowieża, pp. 413–423.
27. Meissner M. (2016b), Wave-based method for simulating small room acoustics, *Progress of Acoustics*, Polish Acoustical Society, Warsaw Division, Warszawa–Białowieża, pp. 425–436.
28. Piechowicz J., Czajka I. (2012), Estimation of acoustic impedance for surfaces delimiting the volume of an enclosed space, *Archives of Acoustics*, **37**(1): 97–102.
29. Pilch A., Kamisiński T. (2011), The effect of geometrical and material modification of sound diffusers on their acoustic parameters, *Archives of Acoustics*, **36**(4): 955–966.
30. Prędka E. (2016), Nonsingular MLM via the multiquadratic RBF in an acoustic indoor problem, *Open Seminar on Acoustics*, Warszawa–Białowieża, pp. 437–440.
31. Rindel J.H. (2010), Room acoustic prediction modeling, *XXIII Encontro Da Socieda de Brasileira Deacústica*, Salvador-Ba,18 A21 De Maio De.
32. Rubacha J., Pilch A., Zastawnik M. (2012), Measurements of the sound absorption coefficient of auditorium seats for various geometries of the samples, *Archives of Acoustics*, **37**(4): 483–488.

33. Shojaei A. (2016), A meshless method for unbounded acoustic problems, *The Journal of the Acoustical Society of America*, **139**(5): 2613–2623, doi: 10.1121/1.4948575.

34. Shojaei A., Galvanetto U., Rabczuk T., Jenabi A., Zaccariotto M. (2019), A generalized finite difference method based on the Peridynamic differential operator for the solution of problems in bounded and unbounded domains, *Computer Methods in Applied Mechanics and Engineering*, **343**: 100–126, doi: 10.1016/j.cma.2018.08.033.

35. Shojaei A., Mossaiby F., Zaccariotto M., Galvanetto U. (2019), A local collocation method to construct Dirichlet-type absorbing boundary conditions for transient scalar wave propagation problems, *Computer Methods in Applied Mechanics and Engineering*, **356**, 629–651, doi: 10.1016/j.cma.2019.07.033.

36. Siltanen S., Lokki T., Savioja L. (2010), Rays or waves? Understanding the strengths and weaknesses of computational room acoustics modeling techniques, *Proceedings of the International Symposium on Room Acoustics, ISRA*, 29–31 August 2010, Melbourne, Australia.

37. Sladek V., Sladek J., Tanaka M. (2000), Optimal transformations of the integration variables in computation of singular integrals in BEM, *Journal for Numerical Method in Engineering*, **47**(7): 1263–1283, doi: 10.1002/(SICI)1097-0207(20000310)47:7<1263::AID-NME811>3.0.CO;2-I.

38. Suh J., Nelson P. (1999), Measurement of transient response of rooms and comparison with geometrical acoustic models, *The Journal of the Acoustical Society of America*, **105**(4): 2304–2317, doi: 10.1121/1.426837.